

## Article

# Using Stable Isotope Analyses to Assess the Trophic Ecology of Scleractinian Corals

Michael P. Lesser <sup>1,\*</sup>, Marc Slattery <sup>2</sup> and Keir J. Macartney <sup>1,†</sup><sup>1</sup> Department of Molecular, Cellular and Biomedical Sciences and School of Marine Science and Ocean Engineering, University of New Hampshire, Durham, NH 03824, USA<sup>2</sup> Department of BioMolecular Sciences, Division of Pharmacognosy, University of Mississippi, Oxford, MS 38677, USA

\* Correspondence: mpl@unh.edu

† Present address: School of Earth, Environmental and Marine Sciences, University of Texas Rio Grande Valley, Port Isabel, TX 78958, USA

**Abstract:** Studies on the trophic ecology of scleractinian corals often include stable isotope analyses of tissue and symbiont carbon and nitrogen. These approaches have provided critical insights into the trophic sources and sinks that are essential to understanding larger-scale carbon and nitrogen budgets on coral reefs. While stable isotopes have identified most shallow water (<30 m) corals as mixotrophic, with variable dependencies on autotrophic versus heterotrophic resources, corals in the mesophotic zone (~30–150 m) transition to heterotrophy with increasing depth because of decreased photosynthetic productivity. Recently, these interpretations of the stable isotope data to distinguish between autotrophy and heterotrophy have been criticized because they are confounded by increased nutrients, reverse translocation of photosynthate, and changes in irradiance that do not influence photosynthate translocation. Here we critically examine the studies that support these criticisms and show that they are contextually not relevant to interpreting the transition to heterotrophy in corals from shallow to mesophotic depths. Additionally, new data and a re-analysis of previously published data show that additional information (e.g., skeletal isotopic analysis) improves the interpretation of bulk stable isotope data in determining when a transition from primary dependence on autotrophy to heterotrophy occurs in scleractinian corals.

**Keywords:** corals; stable isotopes; mesophotic zone; productivity; heterotrophy

**Citation:** Lesser, M.P.; Slattery, M.; Macartney, K.J. Using Stable Isotope Analyses to Assess the Trophic Ecology of Scleractinian Corals. *Oceans* **2022**, *3*, 527–545. <https://doi.org/10.3390/oceans3040035>

Academic Editors: Ronald Osinga, Christian Wild, Peter Schupp, Rupert Ormond, Sebastian Ferse and Leila Chapron

Received: 20 August 2022

Accepted: 8 November 2022

Published: 14 November 2022

**Publisher's Note:** MDPI stays neutral with regard to jurisdictional claims in published maps and institutional affiliations.



**Copyright:** © 2022 by the authors. Licensee MDPI, Basel, Switzerland. This article is an open access article distributed under the terms and conditions of the Creative Commons Attribution (CC BY) license (<http://creativecommons.org/licenses/by/4.0/>).

## 1. Introduction

Deep fore-reef communities are now known as mesophotic coral ecosystems (MCEs; ~30–150 m) to distinguish them from both shallow coral reefs (<30 m) and deeper coral reefs below the euphotic zone (>150 m) [1]. Mesophotic reefs are defined as deep fore-reef communities that occur in low-light habitats and are composed of light-dependent scleractinian corals, soft-corals, macroalgae, and sponges [1–3]. While MCEs have been further subdivided into upper (30–60 m) and lower (60–150 m) depth zones [2], other definitions not dependent on depth per se include changes in coral communities with depth, the transition from autotrophy to heterotrophy and the optical properties of the underwater light field that define the middle and bottom of the euphotic zone [3–7].

Changes in solar radiation with increasing depth, both irradiance, and spectral quality, are the primary abiotic factor affecting the productivity and distribution of benthic photosynthetic organisms [8] and scleractinian corals in particular [1,2,9–12]. In addition to changes in the bulk underwater light environment, there are additional changes in the light environment based on reef topography that interact with coral morphology to affect their productivity as depth changes [13,14]. And on smaller spatial scales, we now know that coral skeletal microarchitecture has a significant effect on the ability of scleractinian

corals to acclimatize to low irradiances [15–19]. Studies on the photophysiology of corals from mesophotic habitats show both a decrease in productivity with increasing depth [12,14,20] and increased photoacclimatization when exposed to decreasing and very low (i.e., below the compensation point) irradiances from shallow to mesophotic depths [10,21–25].

Studies on the trophic ecology of mesophotic corals increasingly rely upon using measurements of naturally occurring stable isotopes of carbon ( $\delta^{13}\text{C}$ ) and nitrogen ( $\delta^{15}\text{N}$ ) within the coral tissues and their Symbiodiniaceae symbionts [26]. The use of stable isotopes in studies on corals, and other symbiotic systems, is based on the propensity of biological systems to utilize the lighter isotopes of carbon and nitrogen preferentially over the heavier isotopes [26]. For stable isotopes of carbon and nitrogen, the trophic fractionation is a result of using  $^{12}\text{C}$  over  $^{13}\text{C}$  and  $^{14}\text{N}$  over  $^{15}\text{N}$ , respectively. Additionally, because carbon can come from sources based on autotrophic or heterotrophic fractionation patterns, sources have a specific range of values that can be useful for understanding the trophic ecology of corals. For coral symbioses, the  $\delta^{15}\text{N}$  values of the holobiont vary based on the source of nitrogen (i.e., atmospheric, dissolved, or particulate), which is further complicated by nitrogen recycling between the coral and symbiont compartments [26]. Analyzed separately, the coral and symbiont compartments can provide significantly more information on the trophic ecology, including the degree of heterotrophy, of corals based on both  $\delta^{13}\text{C}$  and  $\delta^{15}\text{N}$  values.

Using stable isotope analyses (SIA), coral holobionts exhibit varying degrees of mixotrophy [27,28], as well as transitions from autotrophy to heterotrophy, as their primary mode of carbon acquisition along environmental gradients (e.g., irradiance) on mesophotic coral reefs [2]. Recent papers [29–31] have suggested that the SIA evidence for the transition from autotrophy to heterotrophy with increasing depth in mesophotic corals is confounded by several factors, including changes in the proximate biochemical composition (i.e., protein, lipids, and carbohydrates) of coral tissues [32], light-dependent rates of fractionation [33], host-symbiont recycling and retention of carbon [34,35], absence of irradiance effects on isotopic values [36], nutrient effects on SIA [37] and changes in Symbiodiniaceae genetics [38]. For corals, it is well known that there are changes in the relative dependency on autotrophy versus heterotrophy based on species differences and changes in the environment [26,27]. In the mesophotic zone, specifically, the attenuation of light is the most significant change in the abiotic environment affecting the photophysiology of corals and their ability to carry out photosynthesis with a net positive gain in carbon [2,13,14]. Along a shallow to mesophotic depth gradient, SIA evidence has shown that corals can shift their trophic reliance on carbon from primarily autotrophic to increasing dependency on heterotrophy as light decreases with increasing depth [39]. The conclusions from Muscatine et al. (1989) [39] were that at increasingly deeper depths where photosynthesis is declining, other  $\delta^{13}\text{C}$  depleted sources of carbon were being acquired by many Caribbean corals, and this could be explained by a larger reliance on heterotrophic feeding.

As discussed above, Kahng et al. [29–31] have stated that SIA results do not support the interpretation of a transition from autotrophy to heterotrophy in mesophotic corals. To support their conclusions, these authors referenced studies that do not provide the appropriate physiological context for interpreting the SIA results of mesophotic corals. These include Wall et al. (2019) [32], where changes in SIA for shallow water corals recovering from thermally induced bleaching were studied. Coral bleaching is an extreme physiological insult with changes at multiple levels in the host and symbionts that has little to do with naturally occurring, non-stressed corals in any reef habitat [40,41], let alone corals from mesophotic habitats. Other studies used by Kahng et al. [29–31] to interpret the SIA of mesophotic corals include Wall et al. (2020) [38], where the SIA of corals with differing Symbiodiniaceae genotypes at less than 6 m depth in a tropical estuary were examined, or the SIA results from Swart et al. (2005) [33] where the change in carbon isotope values of respired  $\text{CO}_2$  for a single species of coral in shallow water was used to calculate a carbon

isotopic fractionation value assuming that respiration in the day was the same as in the night, which is known to be incorrect [42,43], and an experimental study by Tremblay et al. (2015) [35] which showed that host retention of heterotrophically acquired carbon occurs under low irradiances in corals to compensate for lower rates of photoautotrophy and effects SIA values. Ironically, this is analogous to what is observed for mesophotic corals using SIA when samples are collected along the shallow to mesophotic depth gradient as irradiance and productivity decrease with increasing depth and heterotrophy increases [12,44]. Finally, Kahng et al. (2019) [31] stated that nutrients confound the use of skeletal stable carbon isotopes to assess transitions from autotrophy to heterotrophy for the coral *Montastraea cavernosa* as described in Lesser et al. (2010) [12]. The evidence for this comes from a laboratory experiment using high and unbalanced nutrient concentrations that showed a positive correlation between the  $\delta^{13}\text{C}$  values of the host and symbiont with  $\delta^{13}\text{C}$  skeleton values [37]. However, the Tanaka et al. (2017) [37] experiments were conducted at a constant irradiance of  $\sim 200 \mu\text{mol quanta m}^{-2} \text{s}^{-1}$  and incorporated unbalanced nutrient treatments with an N:P ratio of 101 and 63 for the two species of coral tested. These results provide no relevant data to help understand what the effects, if any, of nutrients are on mesophotic corals. In fact, for *M. cavernosa* along a shallow to mesophotic depth gradient [12], the ambient nutrient concentrations and ratios from the Bahamas are below the Redfield ratio of 16 and suggest nutrient limitation, not eutrophic or unbalanced nutrient conditions, even at mesophotic depths (Figure 1). There is no evidence to support the nutrient effects suggested by Kahng et al. (2019) [31] on the SIA results for *M. cavernosa* from shallow to mesophotic depths.

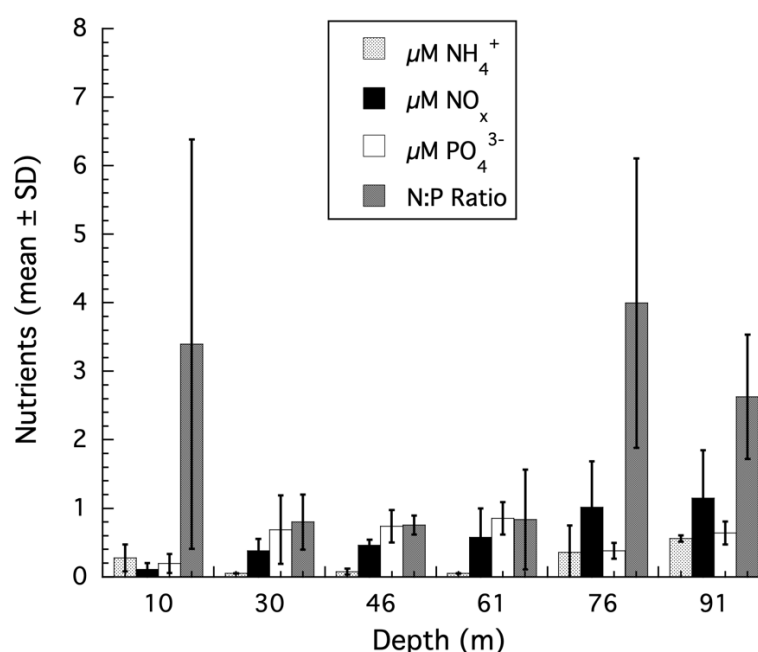


**Figure 1.** Nutrient concentrations from shallow to mesophotic depths using discrete sampling from 10, 30, 46, 61, 76, and 91 m ( $n = 3$  per depth, mean  $\pm$  SD) were collected from the shallow and mesophotic reefs of Bock Wall, Lee Stocking Island, Bahamas and returned to the laboratory where they were immediately filtered using GF/F filters. The seawater filtrate was frozen, transported to the University of New Hampshire (UNH), and analyzed for nitrate/nitrite ( $\text{NO}_x$ ) and ammonium ( $\text{NH}_4^+$ ) and soluble phosphate ( $\text{PO}_4^{3-}$ ) using high throughput colorimetric assays on a Smartchem Chemistry Analyzer at the UNH Water Quality Analysis Laboratory. Nitrogen:phosphorus ratios (N:P) were calculated using the combined  $\text{NO}_x$  and  $\text{NH}_4^+$  concentrations. The  $\text{NO}_x$  data were previously published in Morrow et al. (2016) [45], while the  $\text{PO}_4^{3-}$  and ratio data are published here for the first time.

Additionally, when SIA studies that do involve mesophotic corals are presented as evidence for the lack of any transition to heterotrophy with increasing depth, such as the SIA data in Alamaru et al. (2009) [34], a careful examination of the data actually do support a transition from autotrophy to heterotrophy, contrary to Kahng et al. (2010, 2014, 2019) [29–31], for the coral, *Stylophora pistillata* (see Discussion). In another study by Maier et al. (2010) [36], multiple species from different depths within the genus *Madracis* are combined to cover a shallow to mesophotic gradient with a maximum depth of only 47 m and statistically treated as one species to suggest that increased heterotrophy with depth was not occurring. Given the known variability in SIA values between species [28,39] and that controlling for the effects of these species (i.e., assumption of independence) has been violated, the evidence for the lack of increased heterotrophy with depth is compromised in this case. Another study presented as evidence for the lack of any transition to heterotrophy in mesophotic corals [31] is Crandall et al. (2016) [46], who used bulk  $\delta^{13}\text{C}$  values for coral tissues without separating host from symbionts and compound-specific  $\delta^{13}\text{C}$  values for sterols. Despite the mixed host/symbiont  $\delta^{13}\text{C}$  value, a significant difference between shallow (18–20 m;  $\delta^{13}\text{C} -13.2 \pm 1.2\text{‰}$ ) and mesophotic (55–60 m;  $\delta^{13}\text{C} -17.4 \pm 1.7\text{‰}$ ) colonies of *Montastraea cavernosa* were observed indicating irradiance driven decreases in photoautotrophy for these corals consistent with values previously reported for this species [12]. The values for mesophotic corals, becoming more negative, are approaching the  $\delta^{13}\text{C}$  values for zooplankton, as described above. Additionally, the  $\delta^{13}\text{C}$  values for sterols followed the exact same trend with depth as the bulk isotopic values. Crandall et al. (2016) [46], however, despite the differences in the  $\delta^{13}\text{C}$  values of the bulk tissues and sterols, weigh the lack of differences in sterol composition (e.g., cholesterol) more heavily in their interpretation that no evidence for a transition from autotrophy to heterotrophy is present. Moreover, not having samples of *M. cavernosa* from depths deeper than 60 m limits the ability to detect a transition from autotrophy to heterotrophy relative to the lower mesophotic zone [12].

In addition to the discussion above, several data sets (i.e., case studies) are used, along with new analyses, to assess the utility of SIA to make inferences about the transition from autotrophy to heterotrophy in scleractinian corals from shallow to mesophotic depths. We suggest that multiple lines of evidence, using isotopic and other physiological approaches, should be undertaken to quantify the trophic ecology of mesophotic corals [47], and their potential for increased heterotrophy as irradiance becomes a limiting factor in the mesophotic zone [13,14].

## 2. Materials and Methods

Studies utilizing SIA on scleractinian corals from shallow to mesophotic depths were reanalyzed for evidence of transitions from autotrophy to heterotrophy. Where available, other physiological information (e.g., photosynthesis) as a function of depth was included in the re-analysis and interpretation. The studies on mesophotic corals included SIA data for *Montastraea cavernosa* from the Bahamas [12], *Stylophora pistillata* from the Gulf of Aqaba, Red Sea [44], and *Agaricia lamarki* from the Bay Islands, Honduras [48]. In addition to the  $\delta^{13}\text{C}$  values of the bulk tissues, we re-examined the  $\delta^{15}\text{N}$  values of the bulk tissues and, where available, the  $\delta^{13}\text{C}$  values of the skeleton. Throughout, the following abbreviations will be used  $\delta^{13}\text{C}_{\text{h}}$  = host,  $\delta^{13}\text{C}_{\text{s}}$  = symbiont, and  $\delta^{13}\text{C}_{\text{skel}}$  = skeleton. The application of Stable Isotope Bayesian Ellipses in R (SIBER) to assess isotopic niche width within and between coral species [28,49] was applied, as were  $\delta^{13}\text{C}_{\text{h-s}}$  and  $\delta^{15}\text{N}_{\text{h-s}}$  values to assess the contribution of heterotrophy to coral holobionts over the shallow to mesophotic depth gradient [47]. Additionally, compound-specific  $\delta^{13}\text{C}$  isotopic values for five essential amino acids (CSIA-AA; valine, leucine, isoleucine, methionine, and phenylalanine) were re-examined for *S. pistillata* from the Gulf of Aqaba, Red Sea [50].

### 3. Results

#### 3.1. *Montastraea cavernosa*

The original estimates of gross primary production (GPP) from Lesser et al. (2010) [12] on samples of *Montastraea cavernosa* were made using an optical model of photosynthesis that included the instantaneous downwelling irradiance ( $E_d$ ), the absorption spectrum ( $A$ ), and the quantum yield for photosynthesis ( $\phi_m$ ) as previously described [10,21,51]. The productivity data for *M. cavernosa* are presented as  $\mu\text{mol O}_2 \text{ cm}^{-2} \text{ h}^{-1}$  here. A logarithmic decline of GPP with depth over shallow to mesophotic depths was observed (Figure S1). When log transformed GPP data are plotted, a significant linear decrease with increasing depth is observed (ANOVA:  $F_{1,8} = 832.9$ ,  $p < 0.0001$ ,  $R^2 = 0.99$ , Figure 2A).

A re-analysis of the stable isotope data for *M. cavernosa* using linear regression showed that both the  $\delta^{13}\text{C}$  values of the host fraction (ANOVA:  $F_{1,7} = 27.39$ ,  $p = 0.002$ ,  $R^2 = 0.82$ , Figure 2B) and the symbiont fraction (ANOVA:  $F_{1,7} = 14.37$ ,  $p = 0.009$ ,  $R^2 = 0.71$ , Figure 2B) become increasingly negative with increasing depth. For  $\delta^{15}\text{N}$ , there is no significant effect of depth for the host fraction (ANOVA:  $F_{1,6} = 1.23$ ,  $p = 0.32$ ,  $R^2 = 0.036$ ), or symbiont fraction (ANOVA:  $F_{1,6} = 0.003$ ,  $p = 0.96$ ,  $R^2 = -0.19$ ). Significant depth effects for the  $\delta^{13}\text{C}$  values of the coral skeleton (ANOVA:  $F_{1,6} = 12.21$ ,  $p = 0.017$ ,  $R^2 = 0.65$ , Figure 2C) were observed. There is no significant relationship between the  $\delta^{13}\text{C}$  and  $\delta^{18}\text{O}$  values of the coral skeleton for *M. cavernosa* (Figure S2), indicating metabolic effects on isotopic fractionation dominated as depth increases. The calculation of  $\delta^{13}\text{C}_{\text{h-s}}$  showed a significant decrease with depth (ANOVA:  $F_{1,7} = 13.28$ ,  $p = 0.011$ ,  $R^2 = 0.69$ , Figure 2D) while  $\delta^{15}\text{N}_{\text{h-s}}$  showed no significant effect of depth (ANOVA:  $F_{1,6} = 1.89$ ,  $p = 0.228$ ,  $R^2 = 0.27$ ). A SIBER analysis was also used for the corals described above to assess isotopic niche width (Figure 3). Significant  $p$  values generated from a residual permutation procedure and Hotelling's  $T^2$  test using the standard ellipse area data show that host and symbiont isotopic niches for shallow (3, 10, 15, and 23 m) and upper mesophotic (30 and 46 m) samples of *M. cavernosa* both have a non-significant 53% and 55% overlap indicating that both the host and symbiont occupy similar isotopic niches (Figure 3A,B). In contrast, lower mesophotic samples (61 m) of *M. cavernosa* show a highly significant (Hotelling's  $T^2 = 60.1$ ,  $F = 21.03$ ,  $p < 0.001$ ) lack of overlap (0.0%) between host and symbiont (Figure 3C) indicating significantly different isotopic niches. When all mesophotic samples (30, 46, and 61 m) are analyzed together for *M. cavernosa*, a highly significant difference (Hotelling's  $T^2 = 12.63$ ,  $F = 5.68$ ,  $p = 0.006$ ) is still observed with an overlap of 21.0% between host and symbiont (Figure 3D) compared to shallow samples at 53%.

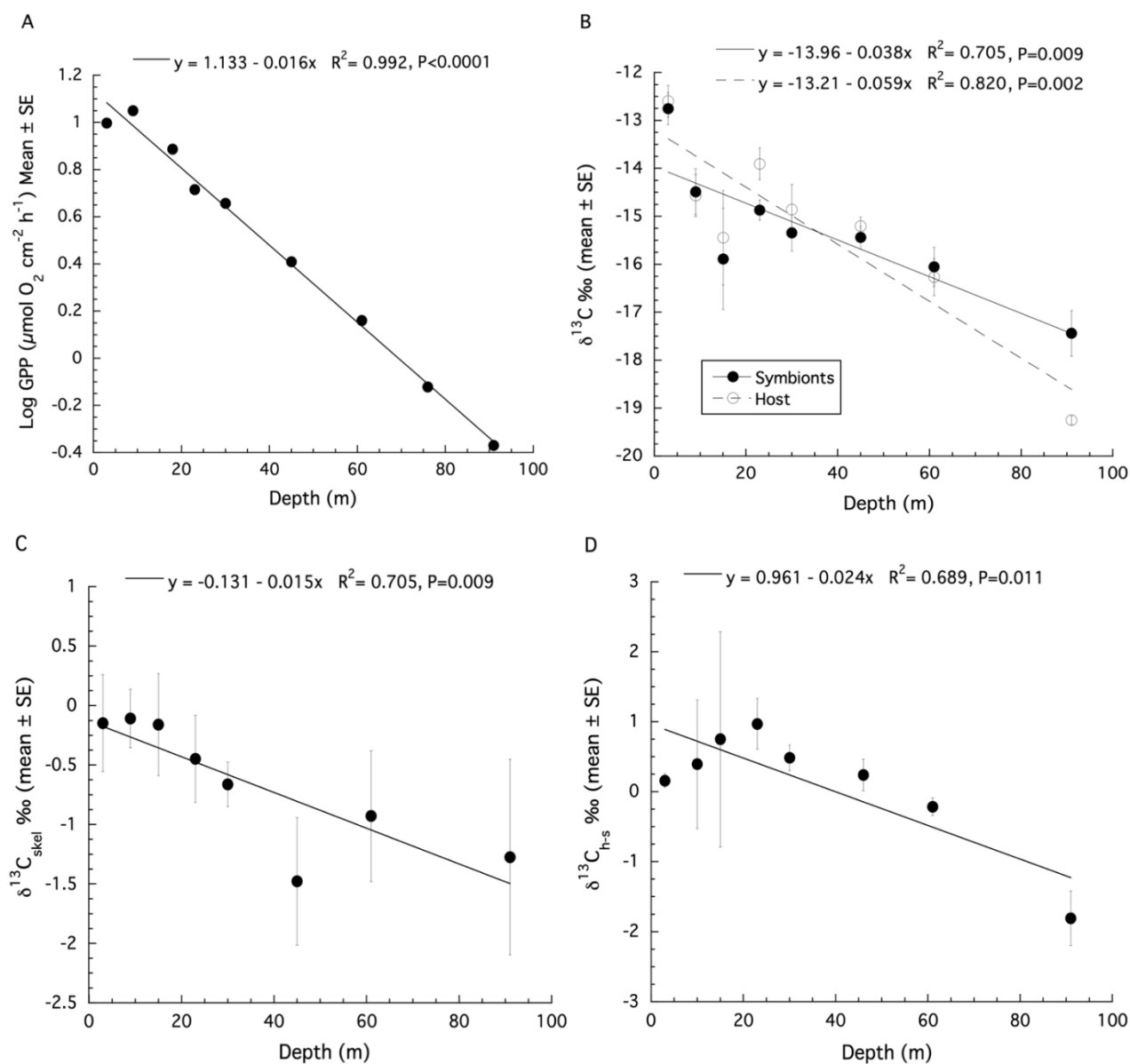


**Figure 2.** (A) Changes in gross primary production (GPP) (mean  $\pm$  SE) with increasing depth for colonies of *Montastraea cavernosa*. (B) Changes in bulk tissue stable  $\delta^{13}\text{C}$  isotopes (mean  $\pm$  SE) for the host and symbiont of *M. cavernosa* with depth. (C) Changes in stable  $\delta^{13}\text{C}$  isotopes (mean  $\pm$  SE) for the skeleton of *M. cavernosa* with depth. (D) Changes in  $\delta^{13}\text{C}_{\text{h-s}}$  (mean  $\pm$  SE) for colonies of *M. cavernosa* with depth.

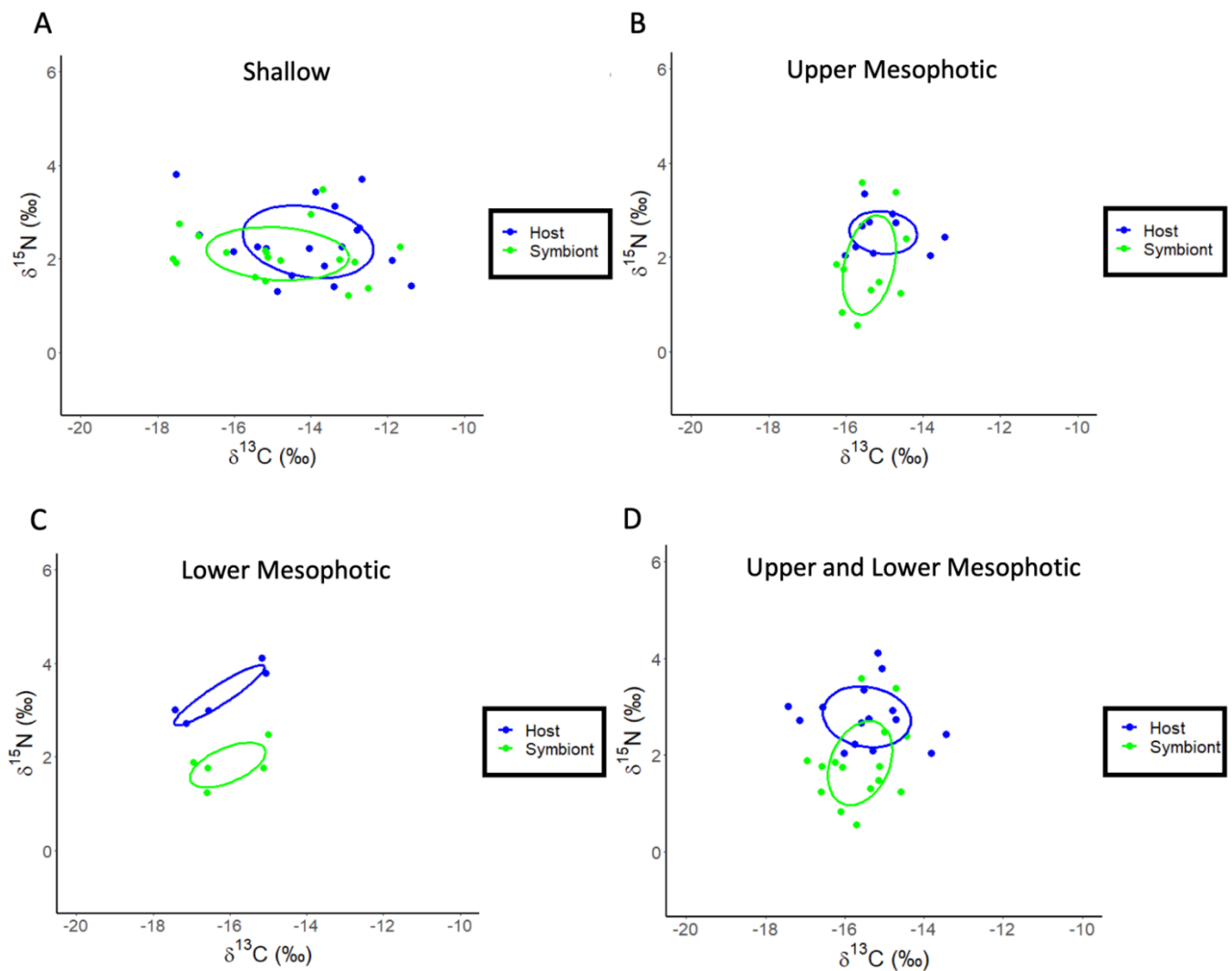


**Figure 3.** SIBER analysis for *Montastraea cavernosa* to assess isotopic niche width. Blue dots represent coral host tissues, while green dots represent symbionts. Dotted lines represent convex hulls which are highly sensitive to sample size, and solid lines represent standard ellipse areas of overlap corrected for sample size (SEAc). (A) Shallow samples of *M. cavernosa*. (B) Upper mesophotic samples of *M. cavernosa*. (C) Lower mesophotic samples of *M. cavernosa*. (D) Upper and lower mesophotic samples of *M. cavernosa* combined.

### 3.2. *Stylophora pistillata*

The re-analysis of the stable isotope data for *Stylophora pistillata* from Einbinder et al. (2009) [44] using linear regression showed that the  $\delta^{13}\text{C}$  values of both the host fraction (ANOVA:  $F_{1,16} = 165.02$ ,  $p < 0.0001$ ,  $R^2 = 0.92$ , Figure 4A) and the symbiont fraction (ANOVA:  $F_{1,16} = 14.37$ ,  $p < 0.0001$ ,  $R^2 = 0.86$ , Figure 4A) become increasingly negative with increasing depth. The calculation of  $\delta^{13}\text{C}_{\text{h-s}}$  showed a significant decrease with depth (ANOVA:  $F_{1,16} = 7.26$ ,  $p = 0.016$ ,  $R^2 = 0.33$ , Figure 4B). For  $\delta^{15}\text{N}$ , there is also a significant effect of depth for the host fraction (ANOVA:  $F_{1,16} = 8.35$ ,  $p = 0.011$ ,  $R^2 = 0.36$ , Figure 4C) and symbiont fraction (ANOVA:  $F_{1,16} = 16.14$ ,  $p = 0.001$ ,  $R^2 = 0.52$ , Figure 4C) but not for  $\delta^{15}\text{N}_{\text{h-s}}$  (ANOVA:  $F_{1,16} = 0.25$ ,  $p = 0.620$ ,  $R^2 = 0.02$ ). The SIBER analysis of these data shows that the host and symbiont compartments for both shallow (5, 10, 15, and 20 m) (Hotelling's  $T^2 = 95.9$ ,  $F = 38.94$ ,  $p < 0.001$ ) and mesophotic (30, 50 and 65 m) samples of *S. pistillata* occupy significantly (Hotelling's  $T^2 = 38.49$ ,  $F = 16.04$ ,  $p < 0.001$ ) different (0.0% overlap) isotopic niches (Figure 5A,B).

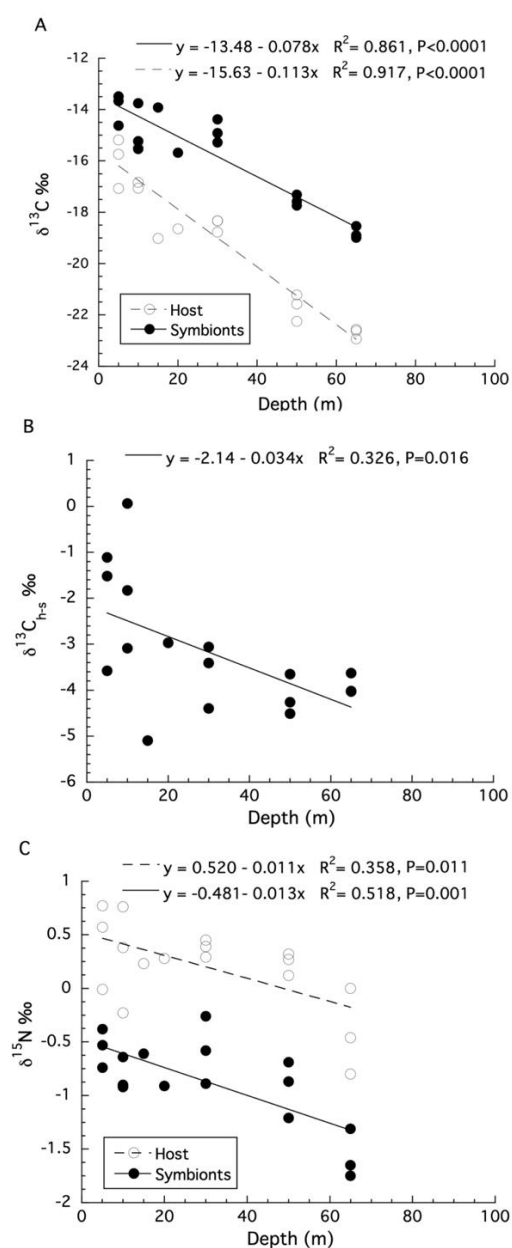


**Figure 4.** (A) Changes in bulk tissue stable  $\delta^{13}\text{C}$  isotopes for the host and symbiont compartments of *Stylophora pistillata* with depth. (B) Changes in  $\delta^{13}\text{C}_{\text{h-s}}$  for colonies of *S. pistillata* with depth. (C) Changes in stable  $\delta^{15}\text{N}$  isotopes for the host and symbiont of *S. pistillata* with depth.



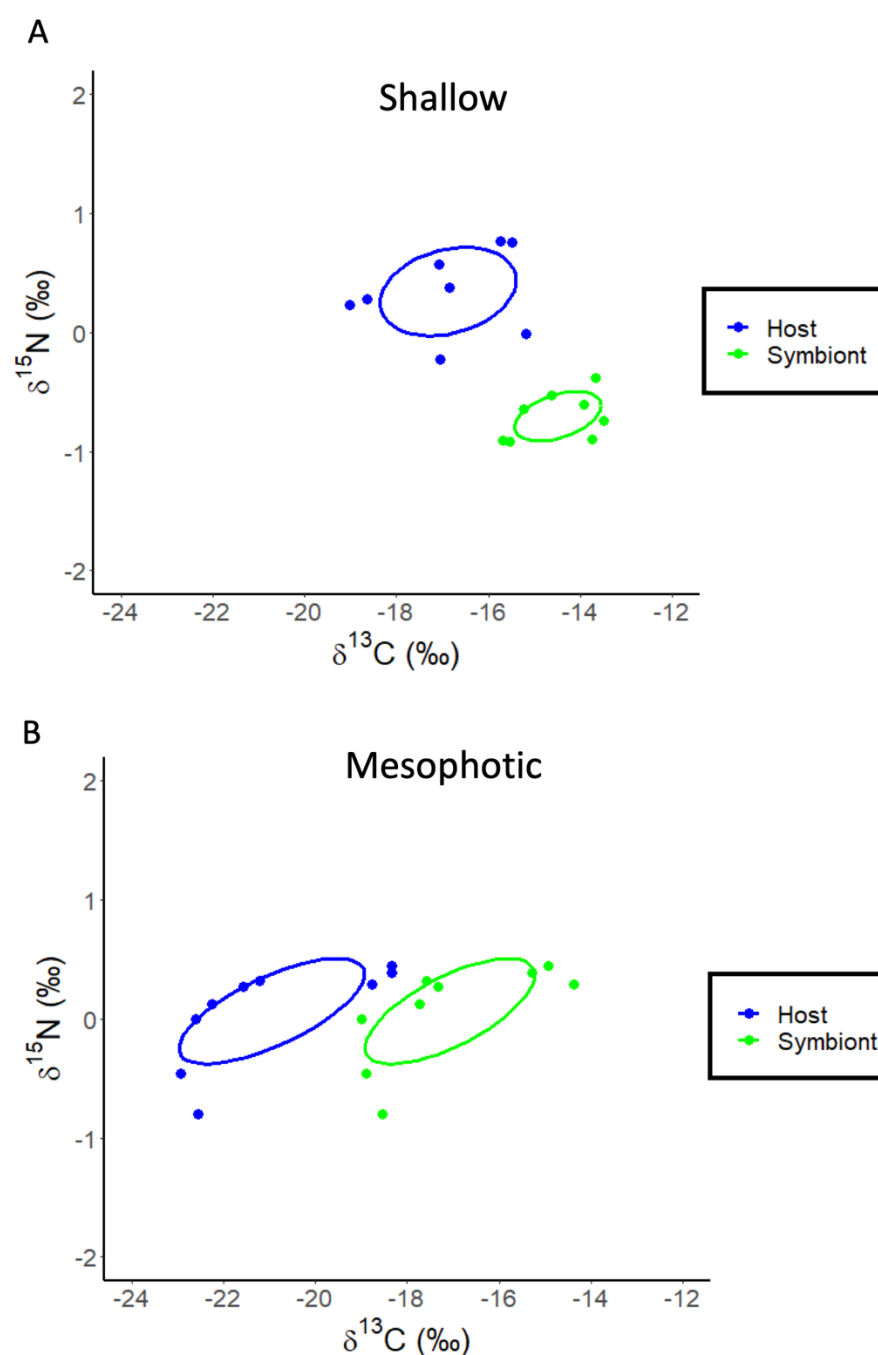


**Figure 5.** SIBER analysis for *Stylophora pistillata* to assess isotopic niche width. Blue dots represent coral host tissues, while green dots represent symbionts. Dotted lines represent convex hulls which are highly sensitive to sample size, and solid lines represent standard ellipse areas of overlap corrected for sample size (SEAc). (A) Shallow samples of *S. pistillata*. (B) Mesophotic samples of *S. pistillata*.

### 3.3. *Agaricia lamarki*

The SIA data for *Agaricia lamarki* are limited because the separation of the symbiont from the host compartments was not conducted [48]. There were two sites used to collect samples along different depth ranges with no measurements of irradiance for these sites. Moreover, measurements of the  $\delta^{15}\text{N}$  of the sediments were not significantly different between sites, and the ANCOVA analysis for the  $\delta^{13}\text{C}$  values of dissolved inorganic carbon (DIC) from the water column does not meet two requirements of an ANCOVA: a significant linear regression of  $\delta^{13}\text{C}$  DIC with depth for both locations, and homogeneity of their

slopes (see Figure S4 in Laverick et al. (2019) [48]). This appears to be the case for several of the analyses presented (see SIA panels Figure 1 in Laverick et al. (2019) [48]). Because these designated site characteristics were not significantly different between sites (see Figure 3 in Laverick et al. [48]), the data for the two sites are analyzed together here. Linear regression showed no significant effect of depth on the  $\delta^{13}\text{C}$  values (ANOVA:  $F_{1,98} = 1.28$ ,  $p = 0.259$ ,  $R^2 = 0.013$ , Figure 6A) or  $\delta^{15}\text{N}$  values (ANOVA:  $F_{1,98} = 0.93$ ,  $p = 0.337$ ,  $R^2 = 0.009$ , Figure 6B) for the holobiont. Significant depth effects for  $\delta^{13}\text{C}$  values of the coral skeleton (ANOVA:  $F_{1,98} = 38.95$ ,  $p < 0.0001$ ,  $R^2 = 0.282$ , Figure 6C) were observed. In what appears to be a correction for the kinetic effects observed in Figure 6C, the skeletal  $\delta^{13}\text{C}$  values were subtracted from the holobiont  $\delta^{13}\text{C}$  values [48]. The resulting data, known as the tissue “ $\delta^{13}\text{C}$  differential”, reportedly represents the long-term photosynthetic activity of corals at each depth (i.e., metabolic effects) and does show a significant decrease with increasing depth (ANOVA:  $F_{1,98} = 38.95$ ,  $p < 0.0001$ ,  $R^2 = 0.282$ , Figure 6C). All data used here can be found in the supplemental files from Laverick et al. [48].

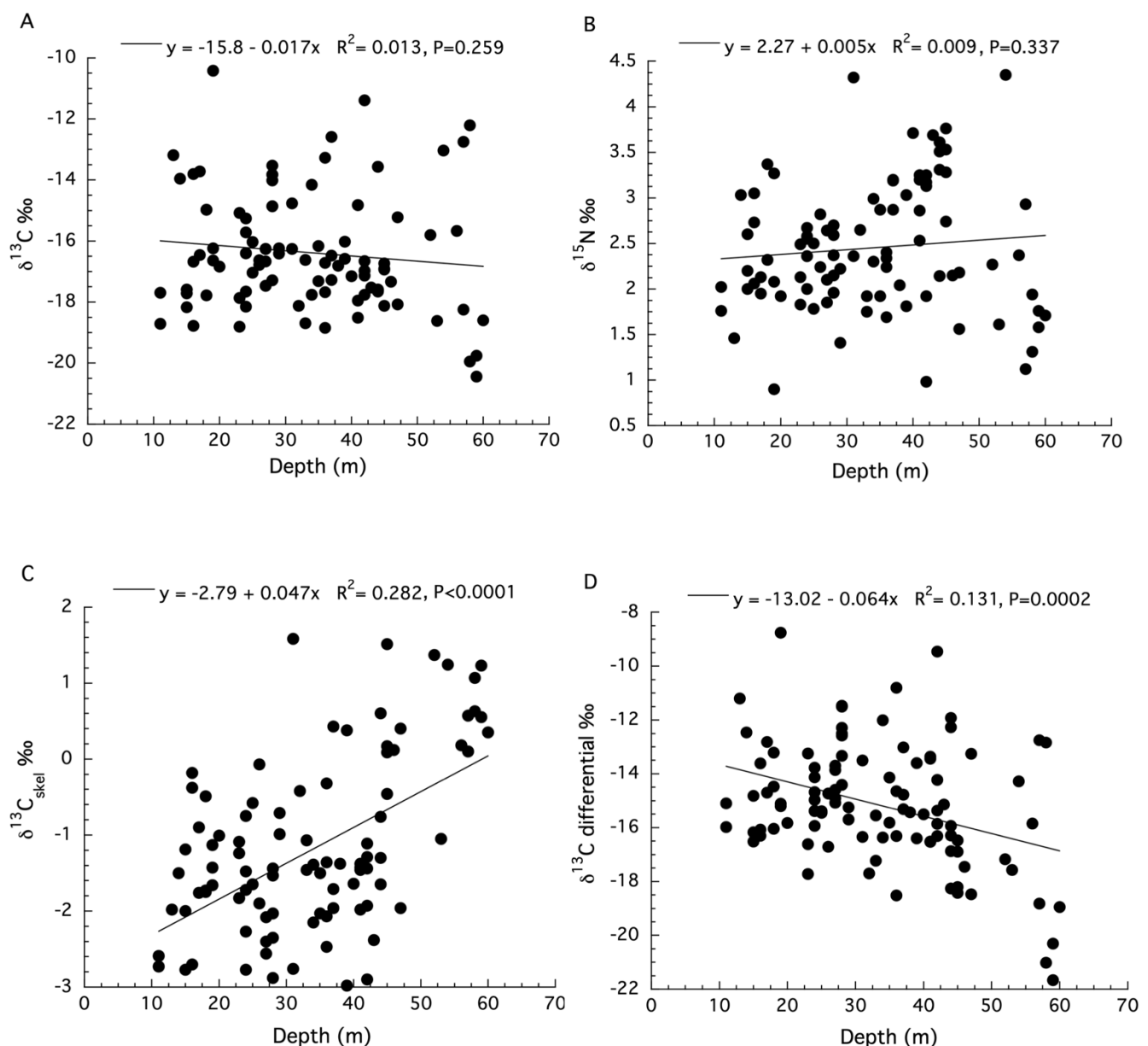


**Figure 6.** (A) Changes in bulk tissue stable  $\delta^{13}\text{C}$  isotopes for the holobiont of *Agaricia lamarki* with depth. (B) Changes in stable  $\delta^{15}\text{N}$  isotopes for the holobiont of *A. lamarki* with depth. (C) Changes

in stable  $\delta^{13}\text{C}$  isotopes for the skeleton of *A. lamarki* with depth. **(D)** Changes in the stable  $\delta^{13}\text{C}$  differential for colonies of *A. lamarki* with depth.

### 3.4. Compound-Specific Isotopic Analysis of Amino Acids (CSIA-AA) for *Stylophora pistillata*

For the CSIA-AA on *Stylophora pistillata* only the samples from the shallow (5 m) and mesophotic (60 m) were re-examined here because the original reciprocal transplant was not fully orthogonal [50] after losing a treatment group, precluding any ecological interpretation of the transplant data and in the absence of statement that a Type III sum of squares was used in the original PERMANOVA analysis. Using a two-way ANOVA, with interaction, for depth and holobiont compartment (i.e., symbiont versus host) for the CSIA-AA values reveals that only the independent factor of depth was significant for all amino acids tested. Collapsing the model to a single factor ANOVA for depth showed that there are no unequal variances using Levene's test, and the data are normally distributed based on a Goodness-of-Fit test for all amino acids examined. Only two amino acids, valine (ANOVA:  $F_{1,21} = 4.91$ ,  $p = 0.038$ ) and isoleucine (ANOVA:  $F_{1,21} = 5.97$ ,  $p = 0.024$ ) showed a significant effect of depth, with shallow corals having less negative  $\delta^{13}\text{C}$  values than their mesophotic counterparts, with methionine being the only exception (Figure 7). Unlike the CSIA-AA analyses, where only depth had a significant effect on the  $\delta^{13}\text{C}$  values of the amino acids, an analysis of trophic position (TP) based on the CSIA-AA of glutamic acid and phenylalanine as described by Martinez et al. (2020) [50], reveals no effect of depth or interaction between depth and compartment, but significant differences between the host and symbiont compartments for all coral samples (ANOVA:  $F_{1,16} = 13.46$ ,  $p = 0.002$ ) with a mean TP for symbionts of  $1.32 (\pm 0.05 \text{ SE})$  and  $1.65 (\pm 0.07 \text{ SE})$  for the host. Using the TP data to calculate the percent heterotrophic contribution to the holobiont as previously described [52,53], there is no significant effect of depth (ANOVA:  $F_{1,8} = 0.289$ ,  $p = 0.605$ ) on the contribution of primary producers (i.e., phytoplankton, autotrophic picoplankton) as well as particulate organic matter (POM) at 5 m ( $47.4\% \pm 5.6 [\text{SE}]$ ) and 65 m ( $41.0\% \pm 10.5 [\text{SE}]$ ), or the contribution of zooplankton (ANOVA:  $F_{1,8} = 0.0006$ ,  $p = 0.981$ ) from 5 m ( $18.9\% \pm 2.7 [\text{SE}]$ ) and 65 m ( $18.8\% \pm 3.7 [\text{SE}]$ ), in their contribution to heterotrophic feeding by the holobiont. All original data used here can be found in the supplemental files from Martinez et al. (2020) [50].

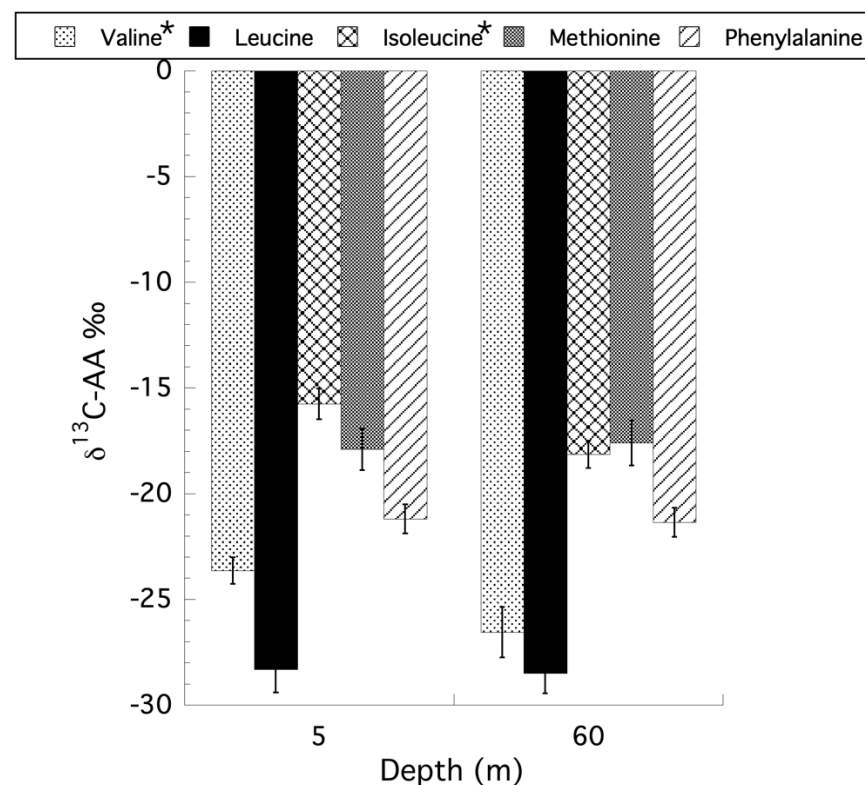


**Figure 7.** Changes in  $\delta^{13}\text{C}$  values for the CSIA amino acid analysis of valine, leucine, isoleucine, methionine, and phenylalanine for samples of *Stylophora pistillata* from 5 and 60 m. \* indicates significant differences between depths for specific amino acids ( $p < 0.5$ ).

## 4. Discussion

### 4.1. The Case for Heterotrophy in Mesophotic Corals

In the mesophotic zone, the attenuation of light is the most significant change in the abiotic environment affecting the physiology of corals [1,2,13,14]. It then follows that the ability of a coral to photosynthesize in the mesophotic zone will affect the reliance of corals on other trophic strategies, such as heterotrophy, to meet their overall metabolic costs for growth with subsequent effects on their distribution and abundance [11,39]. In recent review papers by Kahng et al. (2010, 2014, 2019) [29–31], it was suggested that the SIA data for scleractinian corals are unable to determine if and when the transition from autotrophy to heterotrophy with increasing depth occurs. Here, we have provided a quantitative discussion of the issues, using various sources of SIA data, for several coral species that span the shallow to mesophotic depth gradient. These data show, with high confidence, that these transitions occur in mesophotic corals but that multiple “layers” of evidence are needed to support the conclusion that corals exhibit an increased dependence on heterotrophy with increasing depth. Confounding this is the fact that most scleractinian corals are already mixotrophic and depend on heterotrophy for varying amounts of their carbon and nitrogen requirements, and trophic position is both species and environment dependent [26,27]. Corals can shift their trophic reliance from being primarily autotrophic to a greater dependence on heterotrophy for their carbon requirements as light decreases with increasing depth by exploiting this mixotrophic strategy to suit their species-dependent phenotypes as originally recognized by Muscatine et al. (1989) [39]. This seminal paper, which solidified the use of stable isotope data as a diagnostic marker of trophic status in corals, suggested that the increasingly depleted  $\delta^{13}\text{C}$  signature of the animal tissue of corals, and its divergence from the  $\delta^{13}\text{C}$  of their zooxanthellae, was evidence of increasing heterotrophy in the presence of continued translocation of photosynthate down to a depth of 50 m. Simply put, Muscatine et al. (1989) [39] stated that other  $\delta^{13}\text{C}$  depleted sources of

carbon were increasingly being acquired by many Caribbean corals as depth increased, and this could be explained by a larger reliance on feeding on zooplankton ( $\delta^{13}\text{C}$  values of  $-18.0$  to  $-19.8\text{‰}$ ; [54]) and POM ( $\delta^{13}\text{C}$  values of  $-17.8$  to  $-27.7\text{‰}$ ; [55]). The values for animal tissue in several of the corals from 50 m, examined by Muscatine et al. (1989) [39], were consistent with these values for zooplankton or POM.

The SIA of the Caribbean coral, *Montastraea cavernosa* provides strong evidence for the transition to heterotrophy using the isotopic values from the host, symbiont, and skeletal compartments [12]. First, *M. cavernosa* shows a significant decline in GPP with increasing depth, and the photoautotrophic carbon inputs into colonies as irradiance declines. Additionally, the host, symbiont, and skeleton  $\delta^{13}\text{C}$  values become increasingly negative with depth. Given that there was no significant relationship between the  $\delta^{18}\text{O}$  and  $\delta^{13}\text{C}$  values of the coral skeletons with depth, it is highly unlikely that kinetic effects were overwhelming metabolic effects [56]. Additionally, the crossover depth between the host and symbiont  $\delta^{13}\text{C}$  regression lines occurs in the upper mesophotic zone at  $\sim 40$  m, and the differences between  $\delta^{13}\text{C}$  values of the host and symbionts with depth continue from that depth (i.e.,  $\delta^{13}\text{C}_{\text{h-s}}$ ). A similar pattern was observed for the SIA analysis of the ubiquitous, light-limited, *Leptoseris* spp. complex in the lower mesophotic (i.e., 60–132 m) of the Au‘au Channel (Maui, Hawai‘i), where irradiances decreased from  $\sim 55\text{--}7\ \mu\text{mol quanta m}^{-2}\text{ s}^{-1}$  [23]. The data for *M. cavernosa* also agrees with the isotopic niche width (i.e., SIBER) analysis of  $\delta^{13}\text{C}$  and  $\delta^{15}\text{N}$  values for this coral and support an increasing dependence on heterotrophy along the shallow to mesophotic depth gradient. Surprisingly, for  $\delta^{15}\text{N}$ , there was no significant effect of depth for the host or symbiont fraction, as well as  $\delta^{15}\text{N}_{\text{h-s}}$  values, given the known effects of irradiance on  $\delta^{15}\text{N}$  values in corals [57]. The higher nitrogen isotopic values of the coral tissues compared to its symbionts were, however, consistent with the recycling of internal ammonia and amino acids between the host and Symbiodiniaceae and the associated metabolic fractionation that occurs [58–60]. Additionally, the nitrogen cycle within corals (i.e., nitrogen fixation, nitrification, denitrification, and dissimilatory nitrate reduction) is facilitated by the prokaryotic component of the coral microbiome [61], and for different coral species, nitrogen fluxes within these pathways vary considerably [61]. The species-specific differences in the fluxes within and between these pathways and the recycling of nitrogen within the holobiont have a significant effect on its  $\delta^{15}\text{N}$  values making the interpretation of  $\delta^{15}\text{N}$  values in complex, multi-compartmental symbioses more challenging [62].

Support for the transition to heterotrophy in colonies of *Montastraea cavernosa* also comes from the skeletal  $\delta^{13}\text{C}$  values, which show a significant depletion with increasing depth. Changes in skeletal  $\delta^{13}\text{C}$  values reflect long-term integrated changes in coral metabolism, specifically photosynthesis and respiration, which are affected by the availability of light and heterotrophic food resources such as zooplankton [63–67]. It is widely accepted that skeletal  $\delta^{13}\text{C}$  values reflect changes in the rates of photosynthesis with irradiance and the greater importance of metabolic versus kinetic effects on these values; this relationship varies with coral species and changes in the environment [64,68]. Correction factors for kinetic effects and isotope-based calculations of photosynthesis/respiration (P/R) ratios have been developed and used [64]. Tests of the effectiveness of these correction factors have been reported by Schoepf et al. (2014) [69] using bleached corals. However, using bleached corals to re-evaluate this data correction and to calculate P/R ratios from SIA is not appropriate as coral bleaching, a stress response to elevated temperatures and high solar irradiances, probably affects isotopic fractionation in unknown ways, and likely not in ways related to natural gradients of abiotic factors such as irradiance on shallow to mesophotic coral reefs [40]. Additionally, employing multi-factorial experiments, it was shown in the Hawaiian coral *Porites compressa* that a decrease in irradiance, and therefore photosynthesis, decreases the  $\delta^{13}\text{C}$  values of the skeleton, while increases in the availability and feeding on zooplankton (=brine shrimp) caused an increase in skeletal  $\delta^{13}\text{C}$  values [65]. The increase in skeletal  $\delta^{13}\text{C}$  values is counterintuitive because increasing heterotrophy on zooplankton prey with lower  $\delta^{13}\text{C}$  values should also be reflected as

lower skeletal  $\delta^{13}\text{C}$  values. Grottoli 2002 [65] explains that the effect of increasing food concentration, which significantly increases skeletal  $\delta^{13}\text{C}$  values, is caused by the increased intake of organic nitrogen that increased photosynthesis and  $\delta^{13}\text{C}$  values [27]. However, in the 50% light treatment (i.e., 50% of ambient irradiance in Hawaii), which differed significantly from all other light treatments, only the highest food concentrations were able to counter the effects of lower irradiances on skeletal  $\delta^{13}\text{C}$  values. At the irradiances observed at mesophotic depths [2], the metabolic effects of lower rates of photosynthesis should be even more pronounced. In addition, while all indications are that many scleractinian corals transition to heterotrophy, the concentrations of zooplankton, from the few studies we have in this area, show that zooplankton abundance and biomass, while highly variable, appear to be lower at mesophotic depths compared to shallow depths [70,71]. Lower concentrations of zooplankton at mesophotic depths do not necessarily translate into lower feeding rates at mesophotic depths. In fact, Ezzat et al. (2017) [72] has shown that mesophotic *Stylophora pistillata*, when experimentally provided the same amount of food as shallow water conspecifics, feed at significantly higher rates. There also may be more than enough zooplankton to supply the heterotrophic requirements of the significantly lower population densities of mesophotic corals [12]. This is an area of inquiry that requires more studies to close a large gap in our understanding of heterotrophic feeding by mesophotic corals.

In the SIA study on *Stylophora pistillata* and *Favia fava* from the Red Sea by Alamaru et al. (2009) [34], the  $\delta^{13}\text{C}$  values for the host, symbiont, and symbiont lipids for both corals were significantly different with depth, especially at depths deeper than 15 m. The difference between the animal and zooxanthellae compartments was also significantly different in *S. pistillata* but not in *F. fava*, indicating an increase in the proportion of carbon acquired by heterotrophy for *S. pistillata* as photosynthesis declines, but not for *F. fava*. In this study, the authors used a  $\delta^{13}\text{C}$  cutoff value of  $-21\text{‰}$  for POM that is in the range reported for zooplankton (see above) and the range for host  $\delta^{13}\text{C}$  values at mesophotic depths [34]. Alamaru et al. (2009) [34] also state that the patterns they observed agree with those reported by Muscatine et al. (1989) [39] for Caribbean corals and further state that the observed decrease in  $\delta^{13}\text{C}$  values from 15–60 m is due to the reduction in photosynthesis in both species examined. Using  $\delta^{13}\text{C}$  values for a CSIA-lipid on *S. pistillata* provided strong support for the flow of heterotrophically derived carbon into the lipid fraction of this species below 15 m, while for *F. fava*, the CSIA-lipid  $\delta^{13}\text{C}$  values provide evidence for increased heterotrophy along the entire shallow to mesophotic depth gradient. The differences between these two species are attributed primarily to their morphology and tissue thickness, which in turn affects the degree of diffusion limitation and fractionation of dissolved inorganic carbon species as well as the feeding rates in these corals [34].

In another study of the coral *Stylophora pistillata* from the Red Sea, it was demonstrated that this species can photoacclimatize down to a depth of 65 m, but rates of photosynthesis and calcification still declined significantly with increasing depth [20]. It was concluded that corals at mesophotic depths were obtaining more of their carbon requirements from heterotrophic feeding on zooplankton [20]. This was then followed by an SIA study by Einbinder et al. (2009) [44] on *S. pistillata* from the same location and depth range to discern the trophic status of these corals. They also observed significant differences in both  $\delta^{13}\text{C}_h$  and  $\delta^{13}\text{C}_s$  values with increasing depth, where the host tissue values were significantly more depleted than the symbiont values at depths  $>15\text{ m}$ , as observed by Alamaru et al. (2009) [34]. Einbinder et al. (2009) [44] concluded that because the change in  $\delta^{13}\text{C}$  values “remain constant” with depth in the mesophotic zone, this is evidence for dependence on the same source of carbon by both the host and symbiont and not an increase in heterotrophy. However, the increasing difference in  $\delta^{13}\text{C}$  values between host and symbiont compartments with increasing depth is considered to be a signature of host uncoupling from symbiont photosynthate translocation [39]. Our analysis confirms the significance of the depth-dependent decrease in  $\delta^{13}\text{C}$  values for both the host and symbiont compartments. However, our interpretation of the pattern observed is that as

photosynthesis declines with depth, the amount of translocated carbon from symbiont to host also declines, with the host increasingly dependent on heterotrophically acquired carbon as depth increases. This interpretation is supported by the fact that the slopes for changes in  $\delta^{13}\text{C}_h$  and  $\delta^{13}\text{C}_s$  values with depth diverge with increasing depth and that the  $\delta^{13}\text{C}_h$  values at depths of 50 m and 65 m are consistent with  $\delta^{13}\text{C}$  values reported for zooplankton and POM (see above). Similarly, the SIBER analysis of the isotope data supports this interpretation as the isotopic niche of host and symbionts decreases in their overlap with increasing depth. However, the  $\delta^{15}\text{N}_h$  and  $\delta^{15}\text{N}_s$  values become significantly more negative with increasing depth in this study, and there is no stepwise pattern of isotopic enrichment that would indicate increasing heterotrophy. This pattern is similar to previous studies on *S. pistillata* from the Red Sea [34] and corals from the Caribbean [57,58]. As discussed above, the higher nitrogen isotopic values of the coral tissues compared to its symbionts and the lack of isotopic enrichment is consistent with the recycling of internal ammonia and amino acids between the host and zooxanthellae and the associated changes in metabolic fractionation that occurs as irradiance decreases [57–59]. Overall, this has a significant effect on the  $\delta^{15}\text{N}$  values of the host and symbiont, making the interpretation of  $\delta^{15}\text{N}$  values relative to trophic status more difficult.

In the Caribbean, Laverick et al. (2019) [48] applied SIA to discern the trophic status of *Agaricia lamarki* over a shallow to mesophotic depth range. Here, the shortcoming of using SIA on the bulk coral tissues of the coral holobiont (i.e., without separating host from symbionts) becomes evident as the pattern of  $\delta^{13}\text{C}$  values for the holobiont decrease with increasing depth and  $\delta^{15}\text{N}$  values increase with increasing depth, although neither pattern is significant. While the change in isotopic values with depth for *A. lamarki* appears to indicate increased heterotrophy, interpreting bulk SIA data is difficult without separating the host from symbiont compartments. Additionally, when Laverick et al. (2019) [48] examined skeletal  $\delta^{13}\text{C}$  values, these increased significantly with increasing depth, the opposite pattern expected when there is increased dependence on heterotrophy with increasing depth, except in the presence of very strong kinetic effects [66]. Moreover, the  $\delta^{13}\text{C}$  of DIC varied from  $\sim 0.5$  to  $\sim 1.1\text{‰}$ , which cannot explain the observed increase in  $\delta^{13}\text{C}_{\text{skel}}$  values with depth [66]. In the absence of  $\delta^{18}\text{O}$  skeletal values to apply a known correction for apparent kinetic effects [64], a novel correction of  $\delta^{13}\text{C}_{\text{holobiont}} - \delta^{13}\text{C}_{\text{skel}}$  called the “ $\delta^{13}\text{C}$  differential” was calculated and plotted with depth. This correction resulted in a highly significant, but with a low effect size, decrease in the  $\delta^{13}\text{C}$  differential values with depth, suggesting a decline in photosynthesis with depth. This is similar to the results for *Agaricia agricites* from Jamaica, where the  $\delta^{18}\text{O}$  skeletal correction of Heikoop et al. (2000) [64] was applied. While the physiological basis of the correction applied by Laverick et al. (2019) [48] is not apparent, if it could be experimentally verified, it might be a valuable metric for interpreting coral SIA.

In what many consider to be the most rigorous application of SIA, CSIA-AA provides less ambiguous insights into the trophic biology of corals [73,74]. The analysis of both  $\delta^{15}\text{N}$  (trophic versus source amino acids) and  $\delta^{13}\text{C}$  (essential versus non-essential amino acids) values can be used effectively to unravel trophic sources and sinks with their associated metabolic processes and with better resolution than bulk tissue isotope analysis because the confounding influence of trophic fractionation is largely absent [75–78]. Algae, bacteria, and fungi have highly conserved modes of carbon acquisition and amino acid biosynthesis that produce unique patterns of carbon isotopic fractionation that can be used to “fingerprint” their biosynthetic origin [75,76]. This “fingerprinting” approach and the isotopic fingerprints of different amino acid carbon source end members in CSIA have been shown to be faithfully maintained through a coral reef food web [77,78] and to study the trophic ecology of sponges from shallow to mesophotic depths [79]. Moreover, in consumer tissues, “source” amino acids (e.g., phenylalanine) largely retain the  $\delta^{15}\text{N}$  values of the N sources at the base of the food web, whereas “trophic” amino acids (e.g., glutamic acid) become  $^{15}\text{N}$  enriched by about 7–8‰ per trophic level [80,81]. A key advantage of this technique is that consumer tissue alone is sufficient to derive integrated information

on the  $\delta^{15}\text{N}$  values of the base of the food web as well as the trophic position. Thus, carbon and nitrogen CSIA-AA can provide a significant increase in the power to resolve autotrophy from heterotrophy and trophic position over environmental gradients. The CSIA-AA data from *Stylophora pistillata* [50] shows that of the amino acids studied, mesophotic corals had significantly lower  $\delta^{13}\text{C}$  values for valine and isoleucine compared to shallow corals. These results indicate an increasing dependence on heterotrophic resources with increasing depth. However, both the TP and percent contribution of heterotrophy to the holobiont were not significantly different between depths, and for corals at both 5 m and 60 m, the contribution of heterotrophy, compared to photoautotrophy, to the holobiont is >60%. One possible explanation for this is if the corals analyzed were sampled in winter, when the mixed layer is deep and abundant heterotrophic resources are available, then both shallow and mesophotic corals would have access to abundant food resources (e.g., zooplankton) with lower  $\delta^{13}\text{C}$  values [82].

#### 4.2. Conclusions

With our current understanding of coral trophic biology, it is apparent that species and environmental effects will determine the degree of dependence on heterotrophy for mesophotic corals. It is also evident that multiple types of measurements related to SIA should be employed to provide evidence for the transition to greater dependency on heterotrophy because of the complex nature of changes in physiology with increasing depth and the relationship between the multiple compartments of the coral holobiont. Using studies on changes in stable isotopic values during coral bleaching, using multi-species complexes, or when exposed to eutrophication should not be the basis for understanding the trophic ecology of mesophotic corals as has recently been advocated [29–31]. While gaining increasing traction in the coral reef community because of its sensitivity and specificity, CSIA-AA is expensive, time-consuming and laborious, and largely unavailable to many coral reef biologists. We suggest, at a minimum, that the bulk isotopic values of  $\delta^{13}\text{C}$  and  $\delta^{15}\text{N}$  for both host and symbionts, and food resources, be conducted with the addition of skeletal  $\delta^{13}\text{C}$  and  $\delta^{18}\text{O}$  for the same sample. These measurements will provide insight into the metabolic fractionations over depth while providing insight into kinetic effects that might be masking metabolic effects of interest. The data can also be used in calculating various metrics (e.g.,  $\delta^{13}\text{C}_{\text{h-s}}$ ) and utilized in different modeling frameworks (e.g., SI-BER) to further understand the trophic relationship between host and symbiont as well as changes in the trophic ecology of corals with depth [26,28,47]. Additionally, whether isotopic studies are conducted on shallow or mesophotic corals or on the effects of coral bleaching, the acquisition of SIA results for a wide range of coral species from multiple environments and geographic locations is needed to provide a comparative database. This would allow investigators to contextualize and compare results for specific and similar environmental circumstances and not use changes, for instance, in isotopic values of bleached corals, as a proxy for interpreting the isotopic values of mesophotic corals. These isotopic measurements and analytical approaches should be a component of all studies on the trophic ecology of both shallow and mesophotic corals to provide the context-dependent underpinnings for interpreting transitions from autotrophy to heterotrophy on mesophotic corals and other functional groups on coral reefs, as well as changes in food web structure of coral communities in the Anthropocene.

**Supplementary Materials:** The following supporting information can be downloaded at: <https://www.mdpi.com/article/10.3390/oceans3040035/s1>, Figure S1, Figure S2.

**Author Contributions:** M.P.L. and M.S. designed the research. M.P.L. and K.J.M. analyzed the data. M.P.L., M.S., and K.J.M. wrote and reviewed the manuscript. All authors have read and agreed to the published version of the manuscript.

**Funding:** Support for this research was provided by the National Science Foundation Biological Oceanography program OCE-1437054 to MPL, OCE-1632348/1632333 to MPL and MS, respectively, and the Dimensions of Biodiversity program (OCE-1638296/1638289) to MPL and MS, respectively.



**Institutional Review Board Statement:** Not applicable.

**Informed Consent Statement:** Not applicable.

**Data Availability Statement:** The data analyzed and presented is available as online material, or by request of the contact author, from each of the studies utilized.

**Acknowledgments:** Tali Mass graciously provided the unpublished stable  $\delta^{15}\text{N}$  isotope data for *Stylophora pistillata*.

**Conflicts of Interest:** The authors declare no competing financial interests.

## References

1. Lesser, M.P.; Slattery, M.; Leichter, J.J. Ecology of mesophotic coral reefs. *J. Exp. Mar. Biol. Ecol.* **2009**, *375*, 1–8.
2. Lesser, M.P.; Slattery, M.; Mobley, C.D. Biodiversity and functional ecology of mesophotic coral reefs. *Ann. Rev. Ecol. Syst.* **2018**, *49*, 49–71.
3. Loya, Y.; Eyal, G.; Treibitz, T.; Lesser, M.P.; Appeldoorn, R. Theme section on mesophotic coral ecosystems: Advances in knowledge and future perspectives. *Coral Reefs* **2016**, *35*, 1–9.
4. Laverick, J.H.; Andradi-Brown, D.A.; Rogers, A.D. Using light-dependent scleractinia to define the upper boundary of mesophotic coral ecosystems on the reefs of Utila, Honduras. *PLoS ONE* **2017**, *12*, e0183075.
5. Laverick, J.H.; Tamir, R.; Eyal, G.; Loya, Y. A generalized light-driven model of community transitions along coral reef depth gradients. *Glob. Ecol. Biogeogr.* **2020**, *29*, 1554–1564.
6. Lesser, M.P.; Slattery, M. Will Coral Reef Sponges Be Winners in the Anthropocene? *Glob. Change Biol.* **2020**, *26*, 3202–3211.
7. Tamir, R.; Eyal, G.; Kramer, N.; Laverick, J.H.; Loya, Y. Light environment drives the shallow-to-mesophotic coral community transition. *Ecosphere* **2019**, *10*, e02839.
8. Gattuso, J.-P.; Gentili, B.; Duarte, C.M.; Kleypas, J.A.; Middleburg, J.J.; Antoine, D. Light availability in the coastal ocean: Impact on the distribution of benthic photosynthetic organisms and their contribution to primary production. *Biogeosci.* **2006**, *3*, 489–513.
9. Dustan, P. Depth-dependent photoadaptation by zooxanthellae of the reef coral *Montastrea annularis*. *Mar. Biol.* **1982**, *68*, 253–264.
10. Wyman, K.D.; Dubinsky, Z.; Porter, J.W.; Falkowski, P.G. Light absorption and utilization among hermatypic corals: A study in Jamaica, West Indies. *Mar. Biol.* **1987**, *96*, 283–292.
11. Falkowski, P.G.; Jokiel, P.L.; Kinzie, R.A., III. Irradiance and Corals. In *Coral Reefs. Ecosystems of the World*; Dubinsky, Z., Ed.; Elsevier, Amsterdam, 1990; Volume 25, pp. 89–107.
12. Lesser, M.P.; Slattery, M.; Stat, M.; Ojimi, M.; Gates, R.D.; Grottoli, A. Photoacclimatization by the coral *Montastraea cavernosa* in the mesophotic zone: Light, food, and genetics. *Ecology* **2010**, *91*, 990–1003.
13. Lesser, M.; Mobley, C.D.; Hedley, J.D.; Slattery, M. Incident light on mesophotic corals is constrained by reef topography and colony morphology. *Mar. Ecol. Prog. Ser.* **2021**, *670*, 49–60.
14. Lesser, M.; Slattery, M.; Mobley, C.D. Incident light and morphology determine coral productivity along a shallow to mesophotic depth gradient. *Ecol. Evol.* **2021**, *11*, 13445–13454.
15. Enríques, S.; Méndez, E.R.; Iglesias-Prieto, R. Multiple scattering on coral skeletons enhances light absorption by symbiotic algae. *Limnol. Oceanogr.* **2005**, *50*, 1025–1032.
16. Enríques, S.; Méndez, E.R.; Hoegh-Guldberg, O.; Iglesias-Prieto, R. Key functional role of the optical properties of coral skeletons in coral ecology and evolution. *Proc. Roy. Soc. B.* **2017**, *284*, 20161667.
17. Kühl, M.; Cohen, Y.; Dalsgaard, T.; Jørgensen, B.B.; Revsbech, N.P. Microenvironment and photosynthesis of zooxanthellae in scleractinian corals studied with microsensors for  $\text{O}_2$ , pH and light. *Mar. Ecol. Prog. Ser.* **1995**, *117*, 159–172.
18. Broderson, K.E.; Lichtenberg, M.; Ralph, P.J.; Kühl, M.; Wangpraseurt, D. Radiative energy budgets reveals high photosynthetic efficiency in symbiont-bearing coral. *J. R. Soc. Interface* **2014**, *11*, 20130997.
19. Wangpraseurt, D.; Larkum, A.W.D.; Ralph, P.J.; Kühl, M. Light gradients and optical microniches in coral tissues. *Front. Microbiol.* **2012**, *3*, 316.
20. Mass, T.; Einbinder, S.; Brokovich, E.; Shashar, N.; Vago, R.; Erez, J.; Dubinsky, Z. Photoacclimation of *Stylophora pistillata* to light extremes: Metabolism and calcification. *Mar. Ecol. Prog. Ser.* **2007**, *334*, 93–102.
21. Lesser, M.P.; Mazel, C.; Phinney, D.; Yentsch, C.S. Light absorption and utilization by colonies of the congeneric hermatypic corals *Montastraea faveolata* and *Montastraea cavernosa*. *Limnol. Oceanogr.* **2000**, *45*, 76–86.
22. Einbinder, S.; Gruber, D.F.; Salomon, E.; Liran, O.; Keren, N.; Tchernov, D. Novel adaptive photosynthetic characteristics of mesophotic symbiotic microalgae within the reef-building coral, *Stylophora pistillata*. *Front. Mar. Sci.* **2016**, *3*, 195.
23. Padilla-Gamiño, J.L.; Roth, M.S.; Rodrigues, L.J.; Bradley, C.J.; Bidigare, R.R.; Gates, R.D.; Smith, C.M.; Spalding, H.L. Ecophysiology of mesophotic reef-building corals in Hawai'i is influenced by symbiont-host associations, photoacclimatization, trophic plasticity, and adaptation. *Limnol. Oceanogr.* **2019**, *64*, 1980–1995.
24. Ben-Zvi, O.; Wangpraseurt, D.; Bronstein, O.; Eyal, G.; Loya, Y. Photosynthesis and bio-optical properties of fluorescent mesophotic corals. *Front. Mar. Sci.* **2021**, *8*, 651601.

25. Kramer, N.; Tamir, R.; Ben-Zvi, O.; Jacques, S.L.; Loya, Y.; Wangpraseurt, D. Efficient light-harvesting of mesophotic corals is facilitated by coral optical traits. *Funct. Ecol.* **2022**, *36*, 406–418.
26. Ferrier-Pagès, C.; Leal, M.G. Stable isotopes as tracers of trophic interactions in mutualistic symbioses. *Ecol. Evol.* **2019**, *9*, 723–740.
27. Houlbrèque, F.; Ferrier-Pagès, C. Heterotrophy in tropical scleractinian corals. *Biol. Rev.* **2009**, *84*, 1–17.
28. Conti-Jerpe, I.E.; Thompson, P.D.; Wong, C.W.M.; Oliveira, N.L.; Duprey, N.N.; Moynihan, M.A.; Baker, D.M. Trophic strategy and bleaching resistance in reef-building corals. *Science Adv.* **2020**, *6*, eaaz5443.
29. Kahng, S.E.; Garcia-Sais, J.R.; Spalding, H.L.; Brokovich, E.; Wagner, D.; Weil, E.; Hinderstein, L.; Toonen, R.J. Community ecology of mesophotic coral reef ecosystems. *Coral Reefs*. **2010**, *29*, 255–275.
30. Kahng, S.E.; Copus, J.M.; Wagner, D. Recent advances in the ecology of mesophotic coral ecosystems (MCEs). *Curr. Opin. Environ. Sustain.* **2014**, *7*, 72–81.
31. Kahng, S.E.; Akkaynak, D.; Shlesinger, T.; Hochberg, E.J.; Wiedenmann, J.; Tamir, R.; Tchernov, D. Light, temperature, photosynthesis, heterotrophy, and the lower depth limits of mesophotic coral ecosystems. In *Mesophotic Coral Ecosystems. Coral Reefs of the World*; Loya, Y., Puglise, K.A., Bridge, T., Eds.; Springer International: Cham, Switzerland, 2019; pp. 801–828.
32. Wall, C.B.; Ritson-Williams, R.; Popp, B.N.; Gates, R.D. Spatial variation in the biochemical and isotopic composition of corals during bleaching and recovery. *Limnol. Oceanogr.* **2019**, *64*, 2011–2028.
33. Swart, P.K.; Szmant, A.; Porter, J.W.; Dodge, R.E.; Tougas, J.I.; Southam, J.R. Isotopic composition of respired carbon dioxide in scleractinian corals: Implications for cycling of organic carbon in corals. *Geochim. Cosmochim. Acta* **2005**, *69*, 1495–1509.
34. Alamaru, A.; Loya, Y.; Brokovich, E.; Yam, R.; Shemesh, A. Carbon and nitrogen utilization in two species of Red Sea corals along a depth gradient: Insights from stable isotope analysis of total organic material and lipids. *Geochim. Cosmochim. Acta* **2009**, *73*, 5333–5342.
35. Tremblay, P.; Maguer, J.F.; Grover, R.; Ferrier-Pagès, C. Trophic dynamics of scleractinian corals: A stable isotope approach. *J. Exp. Biol.* **2015**, *218*, 1223–1234.
36. Maier, C.; Weinbauer, M.G.; Pätzold, J. Stable isotopes reveal limitations in C and N assimilation in the Caribbean reef corals *Madracis auretenra*, *M. carmabi* and *M. formosa*. *Mar. Ecol. Prog. Ser.* **2010**, *412*, 103–112.
37. Tanaka, Y.; Grottoli, A.G.; Matsui, Y.; Suzuki, A.; Sakai, K. Effects of nitrate and phosphate availability on the tissues and carbonate skeleton of scleractinian corals. *Mar. Ecol. Prog. Ser.* **2017**, *570*, 101–112.
38. Wall, C.B.; Kaluhiokalani, M.; Popp, B.N.; Donahue, M.J.; Gates, R.D. Divergent symbiont communities determine the physiology and nutrition of a reef coral across a light-availability gradient. *ISME J.* **2020**, *14*, 945–958.
39. Muscatine, L.; Porter, J.W.; Kaplan, I.R. Resource partitioning by reef corals as determined from stable isotope composition I.  $\delta^{13}\text{C}$  of zooxanthellae and animal tissue versus depth. *Mar. Biol.* **1989**, *100*, 185–193.
40. Lesser, M.P. Oxidative stress in marine environments: Biochemistry and physiological ecology. *Ann Rev. Physiol.* **2006**, *68*, 253–278.
41. Lesser, M.P. Coral bleaching: Causes and mechanisms. In *Coral Reefs: An Ecosystem in Transition*; Dubinsky, Z., Stambler, N., Eds.; Springer: Dordrecht, Netherlands, 2011; pp 405–419.
42. Edmunds, P.J.; Spencer-Davies, P. Post-illumination stimulation of respiration rate in the coral *Porites porites*. *Coral Reefs* **1988**, *7*, 7–9.
43. Schrammeyer, V.; Wangpraseurt, D.; Hill, R.; Kühl, M.; Larkum, A.W.D.; Ralph, P.J. Light respiratory processes and gross photosynthesis in two scleractinian corals. *PLoS ONE* **2014**, *9*, e110814.
44. Einbinder, S.; Mass, T.; Brokovich, E.; Dubinsky, Z.; Erez, J.; Tchernov, D. Changes in morphology and diet of the coral *Stylophora pistillata* along a depth gradient. *Mar. Ecol. Prog. Ser.* **2009**, *381*, 167–174.
45. Morrow, K.M.; Fiore, C.L.; Lesser, M.P. Environmental drivers of microbial community shifts in the giant barrel sponge, *Xestospongia muta*, over a shallow to mesophotic depth gradient. *Environ. Microbiol.* **2016**, *18*, 2025–2038.
46. Crandall, J.B.; Teece, M.A.; Estes, B.A.; Manfrino, C.; Ciesla, J.H. Nutrient acquisition strategies in mesophotic hard corals using compound specific stable isotope analysis of sterols. *J. Exp. Mar. Biol. Ecol.* **2016**, *474*, 133–141.
47. Price, J.T.; McLachlan, R.H.; Jury, C.P.; Toonen, R.J.; Grottoli, A.G. Isotopic approaches to estimating the contribution of heterotrophic sources to Hawaiian corals. *Limnol. Oceanogr.* **2021**, *66*, 2393–2407.
48. Laverick, J.H.; Green, T.K.; Burdett, H.L.; Newton, J.; Rogers, A.D. Depth alone is an inappropriate proxy for physiological change in the mesophotic coral *Agaricia larmarki*. *J. Mar. Biol. Assoc. UK* **2019**, *99*, 1535–1546.
49. Jackson, A.L.; Inger, R.; Parnell, A.C.; Bearhop, S. Comparing isotopic niche widths among and within communities: SIBER—Stable Isotope Bayesian Ellipses in R. *J. Anim. Ecol.* **2011**, *80*, 595–602.
50. Martinez, S.; Kolodny, Y.; Shemesh, E.; Scucchia, F.; Nevo, R.; Levin-Zaidman, S.; Paltiel, Y.; Keren, N.; Tchernov, D.; Mass, T. Energy sources of the depth-generalist mixotrophic coral *Stylophora pistillata*. *Front. Mar. Sci.* **2020**, *7*, 566663.
51. Hochberg, E.J.; Atkinson, M.J. Coral reef benthic productivity based on optical absorbance and light-use efficiency. *Coral Reefs* **2008**, *27*, 49–59.
52. Fujii, T.; Tanaka, Y.; Maki, K.; Saotome, N.; Morimoto, N.; Watanabe, A.; Miyajima, T. Organic carbon and nitrogen isoscapes of reef corals and algal symbionts: Relative influences of environmental gradients and heterotrophy. *Microorganisms* **2020**, *8*, 1221.
53. Wall, C.B.; Wallsgrove, N.J.; Gates, R.D.; Popp, B.N. Amino acid  $\delta^{13}\text{C}$  and  $\delta^{15}\text{N}$  analyses reveal distinct species-specific patterns of trophic plasticity in a marine symbiosis. *Limnol. Oceanogr.* **2021**, *66*, 2033–2050.

54. Land, L.S.; Lang, J.C. On the stable carbon and oxygen isotopic composition of some shallow water, ahermatypic, scleractinian coral skeletons. *Geochim. Cosmochim. Acta* **1977**, *41*, 169–172.
55. van Duyl, F.C.; Mueller, B.; Meesters, E.H. Spatio-temporal variation in stable isotope signatures ( $\delta^{13}\text{C}$  and  $\delta^{15}\text{N}$ ) of sponges on the Saba Bank. *Peer J.* **2018**, *6*, e5460.
56. McConnaughey, T.  $^{13}\text{C}$  and  $^{18}\text{O}$  isotopic disequilibrium in biological carbonates: I. Patterns. *Geochim. Cosmochim. Acta* **1989**, *53*, 151–162.
57. Heikoop, J.M.; Dunn, J.J.; Risk, M.J.; Sandeman, I.M.; Schwarcz, H.P.; Waltho, N. Relationship between light and  $\delta^{15}\text{N}$  of coral tissue: Examples from Jamaica and Zanzibar. *Limnol. Oceanogr.* **1998**, *43*, 909–920.
58. Muscatine, L.; Kaplan, I.R. Resource partitioning by reef corals as determined from stable isotope composition II.  $\delta^{15}\text{N}$  of zooxanthellae and animal tissue versus depth. *Pac. Sci.* **1994**, *48*, 304–312.
59. Swart, P.K.; Saied, A.; Lamb, K. Temporal and spatial variation in the  $\delta^{15}\text{N}$  and  $\delta^{13}\text{C}$  of coral tissue and zooxanthellae in *Montastraea faveolata* collected from the Florida reef tract. *Limnol. Oceanogr.* **2005**, *50*, 1049–1058.
60. Reynaud, S.; Martinez, P.; Houbrèque, F.; Billy, I.; Allemand, D.; Ferrier-Pagès, C. Effect of light and feeding on the nitrogen isotopic composition of a zooxanthellate coral: Role of nitrogen cycling. *Mar. Ecol. Prog. Ser.* **2009**, *393*, 103–110.
61. Glaze, T.D.; Erler, D.V.; Siljanen, M.P. Microbially facilitated nitrogen cycling in tropical corals. *ISME J.* **2021**, *16*, 68–77.
62. Tanaka, Y.; Suzuki, A.; Sakai, K. The stoichiometry of coral-dinoflagellate symbiosis: Carbon and nitrogen cycles are balanced in the recycling and double translocation system. *ISME J.* **2018**, *12*, 860–868.
63. Grotoli, A.G.; Wellington, G.M. Effect of light and zooplankton on skeletal  $\delta^{13}\text{C}$  values in the eastern Pacific corals *Pavona clavus* and *Pavona gigantea*. *Coral Reefs* **1999**, *18*, 29–41.
64. Heikoop, J.M.; Dunn, J.J.; Risk, M.J.; Schwarcz, H.P.; McConnaughey, T.A.; Sandeman, I.M. Separation of kinetic and metabolic isotope effects in carbo-13 records preserved in reef coral skeletons. *Geochim. Cosmochim. Acta* **2000**, *64*, 975–987.
65. Grotoli, A.G. Effect of light and brine shrimp levels on skeletal  $\delta^{13}\text{C}$  values in the Hawaiian coral *Porites compressa*: A tank experiment. *Geochim. Cosmochim. Acta* **2002**, *66*, 1955–1967.
66. Omata, T.; Suzuki, A.; Sato, T.; Minoshima, K.; Nomaru, E.; Murakami, A.; Muruyama, S.; Kawahata, H.; Maruyama, T. Effect of photosynthetic light dosage on carbon isotope composition in the coral skeleton: Long-term culture of *Porites* spp. *J. Geophys. Res.* **2008**, *113*, G02014.
67. Linsley, B.K.; Dunbar, R.B.; Dassié, E.P.; Tangri, N.; Wu, H.C.; Brenner, L.D.; Wellington, G.M. Coral carbon isotope sensitivity to growth rate and water depth with paleo-sea level implications. *Nat. Comm.* **2019**, *10*, 2056.
68. McConnaughey, T.A.; Burdett, J.; Whelan, J.F.; Paull, C.K. Carbon isotopes in biological carbonates: Respiration and photosynthesis. *Geochim. Cosmochim. Acta* **1997**, *61*, 611–622.
69. Schoepf, V.; Levas, S.J.; Rodrigues, L.J.; McBride, M.O.; Aschaffenburg, M.D.; Matsui, Y.; Warner, M.E.; Hughes, A.D.; Grotoli, A.G. Kinetic and metabolic isotope effects in coral skeletal carbon isotopes: A re-evaluation using experimental coral bleaching as a case study. *Geochim. Cosmochim. Acta* **2014**, *146*, 164–178.
70. Andradi-Brown, D.A.; Head, C.E.I.; Exton, D.A.; Hunt, C.L.; Hendrix, A.; Gress, E.; Rogers, A.D. Identifying zooplankton community changes between shallow and upper-mesophotic reefs on Mesoamerican Barrier, Caribbean. *Peer J.* **2017**, *5*, e2853.
71. Sponaugle, S.; Goldstein, E.; Doering, K.; D'Alessandro, E.; Guigand, C.; Cowen, R.K. Near-reef zooplankton differences across depths in a subtropical zone. *J. Plankton Res.* **2021**, *43*, 586–597.
72. Ezzat, L.; Maoz, F.; Maguer, J.-F.; Grover, R.; Ferrier-Pagès, C. Carbon and nitrogen acquisition in shallow and deep holobionts of the scleractinian coral, *Stylophora pistillata*. *Front. Mar. Sci.* **2017**, *4*, 102.
73. Fox, M.D.; Smith, E.A.E.; Smith, J.E.; Newsome, S.D. Trophic plasticity in a common reef-building coral: Insights from  $\delta^{13}\text{C}$  analysis of essential amino acids. *Func. Ecol.* **2019**, *33*, 2203–2214.
74. Ferrier-Pagès, C.; Martinez, S.; Grover, R.; Cybulski, J.; Shemesh, E.; Tchernov, D. Tracing the trophic plasticity of the coral-dinoflagellate symbiosis using amino acid compound-specific stable isotope analysis. *Microorganisms* **2021**, *9*, 182.
75. Larsen, T.; Taylor, D.L.; Leigh, M.B.; O'Brien, D.M. Stable isotope fingerprinting: A novel method for identifying plant, fungal, or bacterial origins of amino acids. *Ecology* **2009**, *90*, 3526–3535.
76. Larsen, T.; Ventura, M.; Andersen, N.; O'Brien, D.M.; Piatkowski, U.; McCarthy, M.D. Tracing carbon sources through aquatic and terrestrial food webs using amino acid stable isotope fingerprinting. *PLoS ONE* **2013**, *8*, e73441.
77. McMahon, K.W.; Thorrold, S.R.; Houghton, L.A.; Berumen, M.L. Tracing carbon flow through coral reef food webs using a compound-specific stable isotope approach. *Oecologia* **2016**, *180*, 809–821.
78. Larsen, T.; Hansen, T.; Dierking, J. Characterizing niche differentiation among marine consumers with amino acid  $\delta^{13}\text{C}$  fingerprinting. *Ecol. Evol.* **2020**, *10*, 7768–7782.
79. Macartney, K.J.; Slattey, M.; Lesser, M.P. Trophic ecology of Caribbean sponges in the mesophotic zone. *Limnol. Oceanogr.* **2021**, *66*, 1113–1124.
80. McClelland, J.W.; Montoya, J.P. Trophic relationships and the nitrogen isotopic composition of amino acids in plankton. *Ecology* **2002**, *83*, 2173–2180.
81. Chikaraishi, Y.; Ogawa, N.O.; Kashiya, Y.; Takano, Y.; Suga, H.; Tomitani, A.; Miyashita, H.; Kitazato, H.; Ohkouchi, N. Determination of aquatic food-web structure based on compound-specific nitrogen isotopic composition of amino acids. *Limnol. Oceanogr. Methods* **2009**, *7*, 740–750.
82. Farstey, V.; Lazar, B.; Genin, A. Expansion and homogeneity of the vertical distribution of zooplankton in a very deep mixed layer. *Mar. Ecol. Prog. Ser.* **2002**, *238*, 91–100.